Eur. Phys. J. D **3**, 179–182 (1998)

THE EUROPEAN PHYSICAL JOURNAL D

VUV–spectroscopy of the plasma light emission generated by the pulsed arc cluster ion source (PACIS)*

K. Seeger, L. Köller, J. Tiggesbäumker[a], and K.-H. Meiwes-Broer

Fachbereich Physik, Universität Rostock, Universitätsplatz 3, 18055 Rostock, Germany

Received: 26 February 1998 / Revised: 12 May 1998 / Accepted: 14 May 1998

Abstract. A pinhole grid spectrometer is used to measure the light emission from the plasma of the pulsed arc cluster ion source (PACIS). Spectra of various metals and carbon have been measured between 20 and 100 nm. In the case of carbon the average electron temperature is estimated to about 0.69 eV. Higher temperatures up to 0.79 eV are measured when inserting seeding gas which flushes the discharge volume with approx. one atmosphere of helium. An operation under this source conditions leads to the generation of an intense charged cluster beam. The application of the source as a bright light source in the VUV region is discussed.

PACS. 36.40.-c Atomic and molecular clusters – 52.70.-m Plasma diagnostic techniques and instrumentation

1 Introduction

Since years the cluster source of the type PACIS [1–4] has been used to produce intense pulsed cluster ion beams in order to investigate electronic properties of metal clusters in a beam [5,6] and on surfaces [7]. In comparison to common laser vaporization sources [8], this setup has the advantage of not using an expensive laser for vaporization. As a matter of fact, however, only little is known about the role of the arc discharge, *e.g.*, the plasma electron temperature T_e on the cluster intensity and cluster formation process. Furthermore, the influence of ions in the plasma on the growth of charged clusters is unknown. To get more insight into these processes we have investigated the light emission from the arc discharge in the VUV region between 20 and 100 nm as a function of the source parameters using a simple spectrometer consisting of a pinhole transmission grid and position sensitive detector.

2 Experimental setup

The experimental setup is shown in Figure 1. It contains the PACIS source chamber (1), a differentially pumped pressure stage (2), the Wiley–McLaren [9] type time-of-flight mass spectrometer (TOF) (3), and the VUV–spectrometer (4).

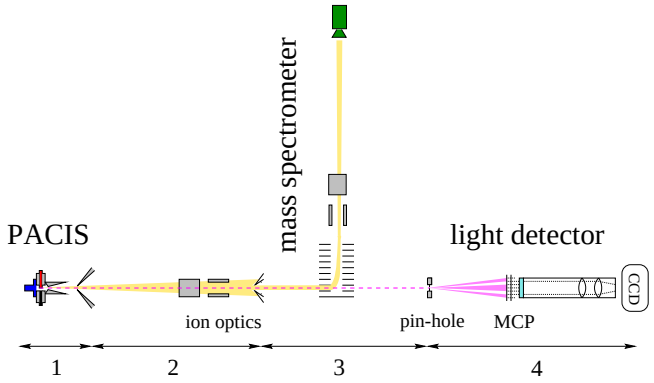

Fig. 1. The experimental setup with the five main parts of the cluster machine: (1) PACIS source chamber; (2) pressure stage with ion optics; (3) TOF mass spectrometer; (5) pinhole CCD spectrometer.

2.1 Pulsed arc cluster ion source

A detailed description of the PACIS is given elsewhere [1,3]. In short: The source contains two metal electrodes separated by approx. 1 mm. The anode is made of stainless steel while the cathode consists of the material which has to be brought into the vapor phase. After flushing of high pressure He through a pulsed solenoid valve (General Valve, Series 9) a pulsed negative voltage (–50 to –1250 V) is applied to the cathode by a home-built pulse generator. During the discharge, atoms, ions, electrons, and photons are produced. Due to the high peak currents (up to 1000 A) and field strength (up to 10 kV/cm) traces of the material are brought into the vapor phase by the spark

* Dedicated to Professor Dr. Hans-O. Lutz on occasion of his 60th birthday

[a] e-mail: josef@mingus.physik2.uni-rostock.de

during the first tens nanoseconds of the discharge. Then arc discharging sets in and the cathode is eroded bringing atoms, ions and electrons into the gas phase. These particles are flushed out of the source chamber by collisions with the carrier gas. While passing a two-side conical channel (ø 1.5−10 mm, 8 cm long) the metal atoms aggregate in order to form clusters. The nascent supersonic beam contains negatively and positively charged clusters as well as neutral species with up to several hundred atoms (N) per cluster.

2.2 VUV-spectrometer

The spectrometer is similar to that used in reference [10] for laser induced plasmas. A pinhole transmission grid (Haidenhein, ø 50 μm, 1000 lines/mm) is located approx. 1 m from the source. A position sensitive detector which consists of a two stage micro-channel plate and a phosphorus screen (Galileo, ø 40 mm) records the diffracted VUV intensity (zero and first order). A voltage of −1.6 kV applied to the plates and 2.5 kV at the anode of the phosphorus screen leads to an amplification of up to 10^6 to 10^8. During the experiment, however, the amplification is kept low in order to avoid saturation effects and to suppress the background. The output of the phosphorus screen is imaged by a two stage telescope onto the array of a slow frame CCD camera (Scientific Instruments, TE/CCD-576E, 576 × 384 pixels, 16 bit dynamic). The distance between pinhole grid and detector (166 mm) is chosen to image the spectra between 20 and 100 nm. The detection probability of the MCP unit (≈ 10%) is nearly constant in this photon energy range.

Absolute wavelength calibration of the detector is achieved by the recording of the He-I (58.43 nm) and He-II (30.38 nm) lines. For this purpose we inject Helium continuously into the source (giving a pressure of 10^{-3} to 10^{-2} mbar in the chamber) and ignite the discharge at 400 V/100 mA. In contrast to this the emission spectra of the other materials were taken in a pulsed mode (10 Hz). Usually the signal is integrated over approx. 100 shots and averaged over 10 CCD pixels perpendicular to the diffraction plane. The resolution of the spectrometer can be estimated to approx. 2 nm.

2.3 Determination of the plasma temperature

For a local thermal equilibrium plasma the average electron temperature T_e (which is an upper limit for the plasma temperature) can be determined using a Boltzmann distribution. In this case we have access to T_e by the intensity ratio I_{jk} of two atomic transitions [11].

$$I_{jk} := \frac{I_{ji}}{I_{ki}} = \frac{g_j}{g_k}\frac{A_{ji}}{A_{ki}}\frac{\nu_{ji}}{\nu_{ki}}\exp(-(E_j - E_k)/kT_e), \qquad (1)$$

where g_x are the statistical weights for the initial and final state, respectively, A_{xy} is the probability for the transition $x \to y$ with the emission of a photon of frequency ν_{xy}, and

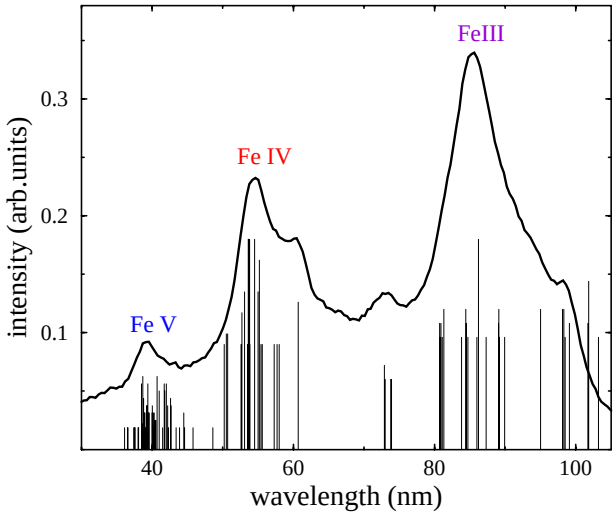

Fig. 2. Light from the PACIS between 30 and 100 nm when operating the source with iron at a discharge voltage of 800 V and a He carrier gas backing pressure of 20 bar, bold curve. The maxima correspond to different ionization stages of atomic iron. The vertical bars mark the positions and intensities of known transitions [13].

$(E_x - E_y)$ corresponds to the energy of the transition. This expression is only valid in the case that the final or the initial states of the two transitions are equal. Alternatively, the plasma temperature could be calculated through the observed ionization states of the atoms by using the Saha-Eggert equation.

3 Results and discussion

A typical spectrum of the PACIS operating with a discharge voltage of about 800 V is shown in Figure 2. Here iron is used as cathode material, with a He seeding gas pressure of 20 bar. Due to the optical response of the MCP detector the spectral range is limited to below 100 nm. The high density of states in these metal ions leads to congested spectra which cannot be resolved with the present setup. However the detection of charge stages up to $z = 4$ (FeV) shows the sensitivity of this method compared to other methods [12]. For comparison, the positions and intensities of the FeIII-V transitions are inserted into the figure [13]. Obviously the observed peaks in the measured spectrum originate from the different ionization steps of the iron atom. Considering the highest ionization stage (FeV) and using the Saha-Eggert equation, we estimate the electron temperature to about 2–5 eV. However, for a calculation of T_e the electron densities (n_e) in the plasma must be known; this we estimate to a typical value [14] of 10^{22} electrons/m^3 (lower n_e implies lower T_e).

In carbon with only 6 electrons per atom the situation appears simpler. Nevertheless, due to fine- and hyperfine splitting of the ground and excited states often several close-lying transitions contribute to one observed emission peak. Figure 3 shows a carbon spectrum generated with the PACIS. As indicated by the symbols (CI:△,

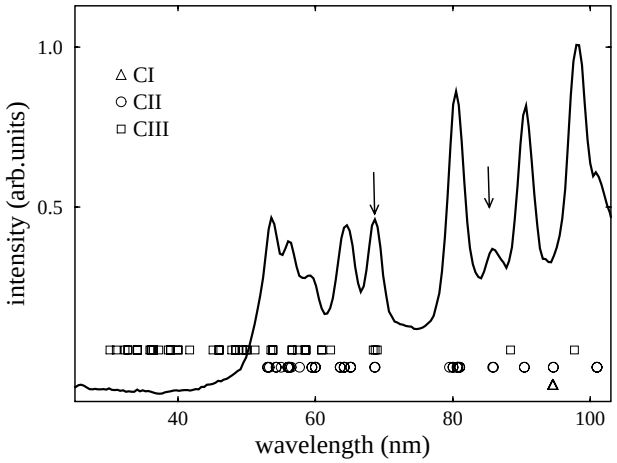

Fig. 3. Carbon VUV spectrum of the PACIS between 30 and 100 nm. Again the known transitions are indicated [15]. For the temperature calculation we use two transitions at 68.7 nm and 85.5 nm (see aroows and Tab. 1). Note the strong drop in intensity close to 50 nm which is due to absorption in the He seeding gas.

Table 1. Initial and final states, the wavelengths, transition probabilities, and statistical weights of the two CII transitions [13,15] used to calculate the electron plasma temperature.

transition	λ_{ik}(nm)	$A(10^8\ \mathrm{s}^{-1})$	g_i	g_k
$2p^2P^o$ - $3s^2S$	85.8	0.369	2	2
$2p^2P^o$ - $3d^2$	68.7	27.0	4	6

CII:▽, CIII:□) the emission mainly results from CII with minor intensities from CI and CIII. Table 1 shows the data needed for the calculation of the electron temperature. From the ratio of two well-resolved peaks from CII transitions (see arrows in Fig. 3 and with Eq. (1)), we calculate a time-averaged electron plasma temperature of 0.79 eV. Without He carrier gas a slightly lower plasma temperature is observed (0.69 eV). It is well known [16–18] that most of the current density is carried by a number of small size cathode spots. Increasing the He gas pressure obviously heats up the spot plasma. However, the gas could also favor the formation of additional cathode spots.

In order to get more insight into the dependence of the cluster formation on the source (and thus the plasma) parameters we run discharges under various source conditions. Figure 4 shows the results for carbon as a function of the discharge voltage U and with He seeding gas. Note the sharp intensity drop at 50 nm arising from the ionization of the dense He gas, which has an ionization potential of 24.6 eV (50.4 nm). This feature has been observed for all materials investigated. Only for iron or in the case of running the source without seeding gas a significant intensity arises below 50 nm. For carbon the electron temperature of 0.75 eV at $U = 500$ V rises by several percent while going to higher discharge voltages. However, without He we observe a lower electron temperature of about 0.69 eV, being nearly constant for all discharge voltages.

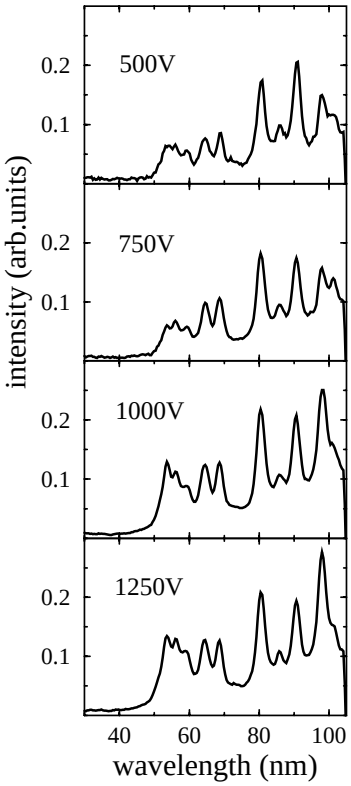

Fig. 4. VUV spectra of carbon for different discharge voltages. The calculated electron temperature (T_e) increase from 0.75 eV up to 0.79 eV at the highest voltage. For details see text.

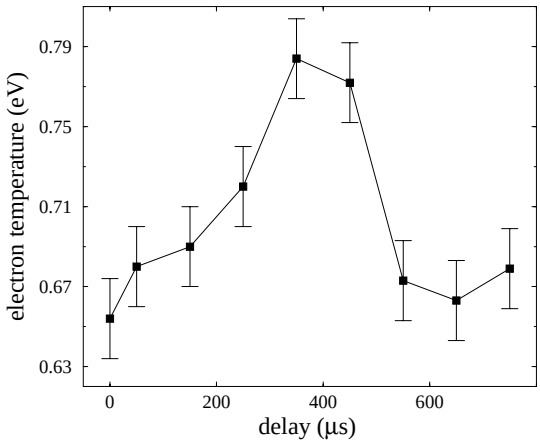

Fig. 5. Variation of the plasma electron temperature T_e for carbon at a different delay between opening of the valve and firing of the discharge.

T_e slightly increases when going to higher He background pressure (up to 25 bar, not shown here). The temperature dependence of the discharge plasma on the He background pressure inside the PACIS can also and more easily be studied by varying the delay between He value opening and firing of the discharge. Here a fixed gas pulse width of 180 μs (adjustment at the valve controller; 20 bar Helium pressure) is used. Figure 5 shows the results again for carbon. Obviously the optimum gas flow is reached after 300 μs. This indicates a value opening time of

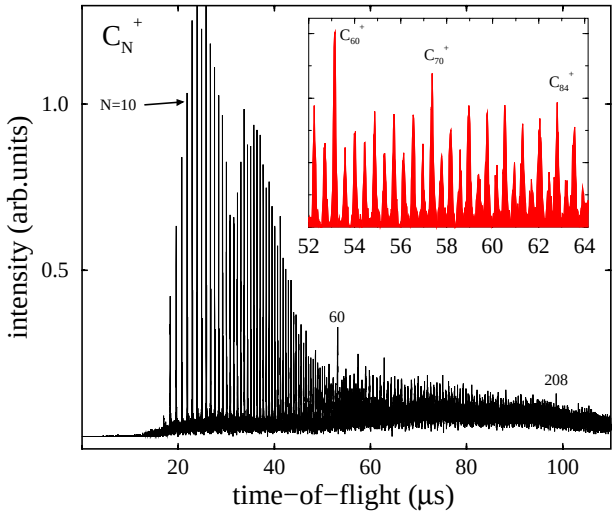

Fig. 6. C_N^+ cluster time-of-flight mass spectrum taken under optimal discharge conditions. The overall shape of the intensity distribution depends on the transmission function and the mass dependent detection efficiency of the spectrometer. Note the higher intensities of the fullerenes C_{60}^+, C_{70}^+ and C_{84}^+ and the even-odd alternation.

approx. 300 μs where T_e is maximum. This indicates that the effective gas pulse is by a factor of 3 longer than the width of the voltage pulse applied to the valve. Another point of interest is the dependence of the growth of the clusters on the plasma parameters. For this reason mass spectra are recorded while varying the delay between gas value opening and the arc trigger. As a general result it can be stated that a source operation at the highest plasma temperature yields the most intense cluster ion emission. Therefore the electron plasma temperature could be taken as an independent cursor for the cluster production efficiency of the source. Figure 6 shows such a time-of-flight $C_N{}^+$ cluster spectrum running under these condition of highest T_e. No multiply charged atoms and clusters have been detected for any of the materials. Thus the higher charged atomic ions seen in the plasma spectra are efficiently neutralized during the aggregation by charge transfer collisions with the gas and the surface. We find that the intensity ratio of positively and negatively charged clusters is close to unit depending slightly on the material used.

Finally the intensity of the VUV light emission has to be addressed. In the case of copper the integrated intensity at a repetition rate of 50 Hz is comparable to the He light source that we used for the calibration of the VUV-spectrometer. Considering a light pulse length of 100 μs the intensity in the PACIS pulse is about a factor of 200 higher than that of the He lamp. In the experiment it turns out that the VUV-light of the PACIS can be used to ionize the residual gas one meter downstream the source.

In summarizing, a simple VUV-spectrometer was used to measure the plasma VUV radiation of the PACIS for various metals and carbon. In the case of carbon strong peaks from CII had been observed and used for the calculation of the plasma temperature. Several variations of different source parameters (with/without seeding gas, different pressure gas, delay between injection of seeding gas and firing of the PACIS) are studied. Upon flushing the source with seeding gas an increase of the electron plasma temperature is observed. Mass spectra recorded with a parameter set that leads to the highest T_e shows the most intense cluster ion production.

Financial support by Deutsche Forschungsgemeinschaft (SFB 198) is gratefully acknowledged. We thank Prof. U. Heinzmann for technical support.

References

1. H.R. Siekmann, Ch. Lüder, J. Faehrmann, H.O. Lutz, K.-H. Meiwes-Broer, Z. Phys. D **20**, 417 (1991); G. Ganteför, H.R. Siekman, H.O. Lutz, K.H. Meiwes-Broer, Chem. Phys. Lett. **165**, 293 (1990).
2. Chia-Yen Cha, G. Ganteför, W. Eberhardt, Rev. Sci. Instr. **63**, 5661 (1992).
3. M. Gausa, R. Kaschner, G. Seifert, J.H. Faehrmann, H.O. Lutz, K.-H. Meiwes-Broer, J. Chem. Phys. **104**, 9719 (1996).
4. W.-Y. Lu, R.-B. Huang, J.-Q. Ding, S.-H. Yang, J. Chem. Phys. **104**, 6577 (1996).
5. R.O. Jones, G. Ganteför, S. Hunsicker, P. Pieperhoff, J. Chem. Phys. **103**, 9549 (1995).
6. P. Milani, M. Ferretti, P. Piseri, C.E. Bottani, A. Ferrari, A. Li Bassi, G. Guizzetti, M. Patrini, J. Appl. Phys. **82**, 5793 (1997)
7. H.R. Siekmann, Bu. Wrenger, E. Holub-Krappe, Ch. Pettenkofer, K.-H. Meiwes-Broer, Z. Phys. D **26**, 54 (1993); A. Bettac, L. Köller, V. Rank, K.H. Meiwes-Broer, Surf. Sci., in press.
8. V.E. Bondeby, J.H. English, J. Chem. Phys. **74**, 6978 (1981); T.G. Dietz, M.A. Duncan, D.E. Powers, R.E. Smalley, J. Chem. Phys. **74**, 6511 (1981).
9. W.C. Wiley, I.H. McLaren, Rev. Sci. Instr. **26**, 1150 (1955).
10. N. Böwering, T. Döhring, U. Gärner, U. Heinzmann, Las. Part. Beams **9**, 593 (1991).
11. H. Drost, *Plasmachemie*, (Akademie-Verlag, Berlin, 1978).
12. E.M. Oks, I.G. Brown, M.R. Dickinson, R.A. MacGill, H. Emig, P. Spädtke, B.H. Wolf, Appl. Phys. Lett. **28**, 711 (1995).
13. R.C. Weast, *Handbook of chemistry and physics*, 66th edn., (CRC Press, Inc., 1985–1986).
14. G. Janzen, *Plasmatechnik*, (Heidelberg, 1992).
15. C.E. Moore, *Tables of Spectra Hydrogen, Carbon, Nitrogen and Oxygen Atoms and Ions*, (CRC Press, Inc., 1993).
16. S. Anders, A. Anders, I. Brown, Rev. Sci. Instr. **65**, 1253 (1994).
17. I.G. Brown, Rev. Sci. Instr. **65**, 3061 (1994).
18. G.W. McClure, J. Appl. Phys. **45**, 2078 (1974).